



poly(pyrrole) films have been obtained from four-point probe measurements on free-standing<sup>14,16</sup> and pressed-pellet films<sup>17</sup>. In dry films, however, the film oxidation state cannot be ascertained by reference to an electrochemical potential. No quantitative data exist for poly(pyrrole), or other conducting polymers to our knowledge, on the conductivity of solvent wetted polymer as a function of potential, or which explore the common presumption that the polymer is equally conducting in the solvent wetted and dry states. Such data, as well as parallel ionic conductivities as a function of potential, are relevant to applications of conducting polymers in solvent-wetted, potential controlled circumstances.

We have described<sup>18</sup> the ionic conductivity of poly(pyrrole) as a function of its oxidation state, and here describe its electrical conductivity, using a modified twin electrode thin layer cell<sup>19</sup>. The poly(pyrrole) film is sandwiched between two Pt working electrodes; the edge of the film is contacted with electrolyte solution through which potential control of the Pt electrodes relative to a reference electrode is attained (Figure 1) The recent poly(pyrrole) coated microelectrode array of Kittleson, et al<sup>10</sup> is also well suited for solvent wetted electrical conductivity measurements.

The capacity of a conducting polymer to store charge is another significant aspect of energy storage use. For poly(pyrrole), charge capacity measurements are also relevant to understanding of its anomalous cyclic voltammetry<sup>14</sup>, which at positive potentials displays a large, capacitor-like "charging" current. This unusual current behavior has been ascribed<sup>13,20</sup> to interfacial (polymer/solution) double layer charging, modeling the poly(pyrrole) as a highly porous electrode material. The enormous surface to

volume ratio required by the double layer charging model<sup>20</sup>, and the task of accounting for optical changes which can be observed in this potential region<sup>18c</sup> and the molecular manner in which interfacial monomer sites would accommodate the charge, are continuing puzzles, however.

Measurement of the poly(pyrrole) charge storing capacity is usually assessed by electrochemical discharge of the polymer by a contacting electrode. In this paper we describe an alternative procedure, "chemical charge assay", using the polymer charge (however stored, whether as a chemical state or as double layer capacitative charge) to oxidize or reduce a solution of a redox titrant contacting the polymer. The chemical charge assay and electrochemical discharge are, ideally, equivalent approaches to measuring poly(pyrrole) charge storing capacity. However, these approaches, in practice, may be non-equivalent if significant heterogeneity in discharge rates exists between different parts (inner, outer, domains, etc.) of the polymer film, since chemical and electrical discharges sample the polymer charge from opposite sides of the film and since a permeating redox titrant may contact charged domains not in good electrical contact with the electrode. This interesting possibility was explored by comparing poly(pyrrole) capacitances obtained by the different approaches.

The chemical charge assay experiment is done in a twin electrode thin layer cell<sup>19</sup>, in which one of the two working electrodes is coated with poly(pyrrole), the other is naked, and they are separated from one another by a thin (10-100 micron) film of solution containing the redox titrant. The polymer film is first charged to a certain potential, and its electrode is then disconnected. The redox titrant is reduced (or oxidized) by the poly(pyrrole) film, and diffuses across the solution cavity to the other

(naked) electrode where it is re-oxidized (or re-reduced) and gives a current flow the integral of which reflects the extent of polymer film discharge. Methyl viologen ( $MV^+$ ) is used as reducing redox titrant for oxidized poly(pyrrole) films, and  $[Ru(bpy)_2Cl_2]^{1+}$  as oxidizing redox titrant for reduced films. The technique is equally applicable to electrically conducting polymers and to "redox" polymers which store charge in well defined redox centers.

The charge assay gives a profile of poly(pyrrole) charge vs. potential, which is correlated with the electrical conductivity profile to obtain an important relation between poly(pyrrole) charge and electrical conductivity.

#### EXPERIMENTAL

Chemicals and equipment. Acetonitrile (Burdick & Jackson) was dried over molecular sieves. Tetraethylammonium perchlorate was recrystallized three times from water. Working electrodes were highly polished (1 micron diamond paste, Buehler) platinum disks. Counter and reference electrodes were Pt coil and Ag/AgCl electrodes, respectively. Potentials are referenced to the NaCl saturated standard calomel electrode (SSCE). Pyrrole (Aldrich) was chromatographed on dry alumina, methyl viologen was used as purchased, and  $[Ru(bpy)_2(Cl)_2]^{22}$  and  $[Os(bpy)_2(vpy)_2](PF_6)_2^{23}$  were synthesized. Electrochemistry was performed with a Pine Instruments ARDE 4 bipotentiostat and a Hewlett Packard 7046A dual pen chart recorder. Electrochemical experiments on poly(pyrrole) were performed in a  $N_2$  atmosphere dry box (Vacuum Atmospheres). Conductive currents were monitored with a Keithly DVM.

Poly(pyrrole) films were prepared by potentiostating the Pt disk at 0.83V vs. SSCE in a pyrrole/0.1 M  $Et_4NClO_4$ /acetonitrile solution. The pyrrole

concentration was chosen to provide a polymerization current density of approximately  $1 \text{ mA/cm}^2$  at this potential. The total charge passed during polymerization was monitored by a locally designed microcomputer, and the polymerization terminated automatically at the desired charge. Poly(pyrrole) film thickness was estimated according to Diaz, et al<sup>15</sup> (1 micron thickness per  $\text{cm}^2$  of electrode area for 240 mC during deposition). These thicknesses were slightly larger than those measured, for thick films, by dislodgement and weighing on a Cahn Model 29 microbalance. ( $d = w/pA$ , where  $d$  is the calculated film thickness,  $w$  is the film weight,  $A$  is the film area, and  $p$  is the reported<sup>2</sup> density of polypyrrole,  $1.48 \text{ g/cm}^3$ ). Poly-[Os(bpy)<sub>2</sub>(vpy)<sub>2</sub>]<sup>2+</sup> films were prepared as reported previously.<sup>22</sup>

Conductivity measurements. The twin electrode thin layer cell, based on a Starrett Model 2A micrometer, used to measure the electrical conductivity of solvent wetted poly(pyrrole) films is shown in Figure 1. Note that the film thickness is grossly exaggerated. For "static" (see below) conductivities, the upper Pt disc electrode was the polished end of an 18 gauge Pt wire (area =  $8 \times 10^{-3} \text{ cm}^2$ ) mounted in a Teflon cylinder fitting snugly onto the micrometer spindle. For "dynamic" measurements, a 36 gauge Pt wire (area =  $3.14 \times 10^{-4} \text{ cm}^2$ ) was sealed in a glass capillary, polished flush, and epoxied into a similar Teflon holder. Electrical contact between the Pt wire electrodes and the micrometer spindle was made with soft (uncured) silver epoxy (Epotek). For both measurements, the lower electrode consisted of a Teflon shrouded Pt disc ( $0.3 \text{ cm}^2$ ) attached to a Starrett 212 adapter and insulated from the body of the micrometer with a slip of Teflon tape. A Teflon cup served as both lower electrode shroud and housing for solution and reference and counter electrodes. A Lucite top limited solvent evaporation from the cup.

For "static" measurements, with the micrometer gap opened wide, the poly(pyrrole) film was grown on the lower (large area) electrode to a 13.9 micron thickness based on the 1.0 C charge passed in polymerization. Such films by weight were 9.6 microns thick, but the electrochemically based<sup>15</sup> thickness was used to calculate conductivity. Replacing the pyrrole solution with fresh 0.1M  $\text{Et}_4\text{NClO}_4$ /acetonitrile, the gap between the two facing electrodes was slowly closed until the resistance between the two working electrodes dropped precipitously, indicating that the upper electrode had contacted the poly(pyrrole). The electrode separation was then slowly decreased further until the resistance stopped decreasing, and the micrometer reading was noted. (The electrode separation could typically be decreased 100 microns from the point of original contact until the resistance minimum was reached. Since final, calculated film thicknesses were 10-15 microns, the film or electrode assemblies must undergo some compression and deformation during this process, probably mostly due to the nonrigid Teflon electrode mounts and uncured silver epoxy contact). Next, the micrometer gap was re-opened (1 mm), and the film potentiostated at the desired potential until the resulting film charging current (rather long lived as the film is rather thick) decayed. (If opening of the gap between the working electrodes was omitted, the film oxidation state responded extremely slowly to changes in electrode potential, showing the importance of facilitating counterion flow into and out of the film.) Maintaining the poly(pyrrole) coated film at the same potential, the two electrodes were then repositioned to the previously noted separation, the naked electrode potential made slightly different (10-100 mV) from the poly(pyrrole) coated electrode, and the resulting current through the film was monitored. This procedure was

followed for a series of film potentials (i.e., a series of film oxidation states).

For "dynamic" experiments the poly(pyrrole) film was grown on the upper, smaller Pt electrode to form a much smaller diameter disk of polymer. The charge passed during polymerization was 1  $\mu\text{C}$ , corresponding to an electrochemically calculated<sup>15</sup> thickness of 13.3 microns. The gap between the electrodes was closed to minimum resistance as above. The electrodes were in this case not subsequently separated. The film oxidation state was changed by slowly scanning the potential of both electrodes, with a constant potential difference (10 mV) between them, relative to a reference electrode.

Chemical Charge Assay Measurements. The cell design was similar to that used for conductivity measurements except that the twin working electrodes were large area (0.25  $\text{cm}^2$ ) Teflon shrouded Pt disks. The auxiliary and reference electrodes are placed in the Teflon solution cup surrounding the electrodes. The twin working electrodes, one polymer coated and the other naked, are separated by a thin solution layer of redox titrant, either  $\text{MV}^{2+}$  or  $[\text{Ru}(\text{bpy})_2\text{Cl}_2]$ . The exact electrode separation was established by plotting the reciprocal of the current flowing between the electrodes due to oxidation and reduction of the redox titrant solution vs. the micrometer setting<sup>19</sup>. If the polymer coated electrode is charged to a potential sufficient to oxidize (or reduce) the redox titrant, the steady-state current between the polymer coated electrode and the naked electrode where the titrant is regenerated, is limited by diffusion of titrant across the thin solution layer. The electron transfer reaction between the polymer coated electrode and the redox titrant was assumed to be confined to the film-solution interface, but the accuracy of this assumption is not particularly crucial to accuracy of the charge

assay.

To assay, for example, the charge stored in (oxidized) poly(pyrrole) at +0.4V, a solution of  $MV^{2+}$  is placed between the electrodes. Potentials of +0.4 and -0.6V are applied to the polymer coated and naked electrodes, respectively, the current due to reduction of  $MV^{2+}$  (at the naked electrode) and oxidation of  $MV^+$  (at the polymer film) allowed to reach steady state, and then, the polymer electrode is disconnected from the bipotentiostat. A current-time transient for  $MV^{2+}$  reduction is obtained at the naked electrode, the integral of which includes the stored charge on the poly(pyrrole) which can be consumed by oxidizing  $MV^+$ . The reaction (ideally) measures the charge required to change the poly(pyrrole) from its initial potential to a potential at or near the formal potential of the  $MV^{2+}/+$  couple. The process is repeated at a series of initial film potentials to give a plot of polymer charge vs. potential.



## RESULTS and DISCUSSION

Electrical Conductivity of Solvent-Wetted Poly(pyrrole). The current passing through the poly(pyrrole) film between the two working electrodes depends on (i) the potential of the poly(pyrrole) coated electrode vs. the reference electrode potential, which determines the polymer oxidation state, and (ii) the potential difference between the two thin layer electrodes, which determines the voltage gradient across the film. The former dependency was previously unknown since the film potential was not controllable in previous<sup>14,16,17</sup> dry state conductivity measurements. Film conductivity values are expressed by:

$$\sigma = dI/AV \quad (1)$$

where  $\sigma$  is film conductivity in  $S\text{ cm}^{-1}$ ,  $d$  is film thickness in  $\text{cm}$ ,  $I$  is the current in amperes between the thin layer electrodes,  $A$  is the area in  $\text{cm}^2$  of the smaller of the two electrodes contacting the film, and  $V$  is the potential difference between the two electrodes.

"Static" measurement (See Experimental) results for poly(pyrrole) are shown in Figure 2 as log conductivity vs. potential. In this experiment, the potential difference between the two electrodes is held constant and the potential vs. the reference electrode is varied, separating the electrodes for a period, at each potential, to allow the film to charge to equilibrium at that potential.

At potentials between +0.4V and 0V, the poly(pyrrole) conductivity is nearly potential-independant, which is interesting in view of the considerable capacity of poly(pyrrole) to store charge in this potential region (see below), and in view of changes in its optical spectrum<sup>18c</sup> which occur here. Our

result, qualitatively, agrees with that of Street, et al<sup>24,25</sup>, who found that dry, reduced poly(pyrrole) reaches a threshold conductivity upon incomplete gas-phase chemical oxidation, indicating that maximum conductivity can be reached before the film is fully oxidatively charged.

The oxidized film conductivity in Figure 2 is significantly lower than the literature value<sup>14</sup> for dry state oxidized poly(pyrrole), 40-100 S cm.<sup>-1</sup>. This difference is not due to the presence of solvent, however, since measurement of the conductivity of a dry film in the twin electrode thin layer cell, followed by addition of solvent and remeasurement, typically gave the same conductivities within a factor of 2x. A similarly low conductivity ( $10^{-2}$  S cm.<sup>-1</sup>) was reported for solvent-wet poly(pyrrole) films attached to a microelectrode array.<sup>10</sup> The reason for the low conductivities is not clear; there may be resistive elements in the electrode/film contact, or the films as we grow them may be less morphologically compact. Whatever the reason, we see no reason to suspect that the relative conductivities observed at different potentials and oxidation states are not meaningful.

At more negative, reducing potentials, the film conductivity becomes strongly potential dependant and drops by approximately 6 orders of magnitude (Figure 2). The film conductivity remains low (confirming Diaz' cyclic voltammetry-based deduction<sup>14</sup>) and nearly constant at about  $10^{-7}$  S cm.<sup>-1</sup>, at strongly negative potentials. The Figure 2 conductivities for highly reduced films should be considered as upper limits, since it is difficult to know how to correct the very small conductive currents measured at these potentials for extraneous background currents, and it is also difficult to know whether the (more resistive) reduced poly(pyrrole) film is truly at equilibrium with the contacting electrode.

Turning now to measurements in which the mean potential of the two electrodes vs. the reference is kept constant, and the potential difference ( $\Delta E$ ) between them is varied (10-100 mV), Figure 3 shows results for log film conductivity  $\sigma$  vs.  $\Delta E$  in a "static" experiment. At potentials between +0.4V and -0.2V, the current varies proportionately to  $\Delta E$ , so the conductivity is constant. Thus, solvent-wet poly(pyrrole) behaves ohmically, paralleling the behavior of dry, oxidized films. Highly reduced (-0.3V to -0.4V) films, on the other hand, do not show perfect ohmic behavior, since  $\sigma$  increases slightly at larger  $\Delta E$ . As noted above, measuring film conductivity for highly reduced poly(pyrrole) entails possible errors due to background currents. Film conductivities obtained at small  $\Delta E$  should be regarded as more nearly correct, but even so probably represent the upper limit of highly reduced film conductivity.

The currents for charging the poly(pyrrole) film to a new potential vs. SSCE are low and decay extremely slowly if the micrometer gap between the twin working electrodes is not opened temporarily, as described in Experimental. Since poly(pyrrole) films act as anion exchange polymers<sup>18</sup>, we interpret this experimental requirement as reflecting the need to move counterions for the charged poly(pyrrole) structure in and out of the film as its oxidation state is changed.<sup>18,26</sup> If the electrodes contact the faces of the film, counterion entry/egress is constrained to occur at the edges of the film of polymer, and counterions must diffuse across the entire radius (3 mm) of the poly(pyrrole) film, a slow process. When the electrode gap is opened so that electrolyte/solvent contacts the entire polymer membrane, however, counterions need only diffuse across the polymer film thickness (13.9 microns). Even then, for the highly reduced films, the time required for current transients to decay

can be as long as 10-20 minutes. Such behavior has important implications for the physical design of poly(pyrrole) and analogous conducting polymer films for use as battery materials, since the rates of discharge (current density) of thick films will almost surely be limited by counterion transport.

Following the above arguments, conductivity/potential profiles should be obtainable without separating the two electrodes if the radius of the polymer film is sufficiently small. This was done by making one of the electrodes the tip of a small (100 microns) radius wire, and growing the film only on this tip. Figure 4 shows a preliminary version of such a "dynamic" experiment. The current-potential profile obtained during a slow, continuous scan of the two working electrode potentials is qualitatively similar to that of Figure 2, except that the change in film conductivity is displaced to more positive potentials, and quantitative information on highly reduced polymer is lost. Upon re-oxidation, the film conductivity returns to nearly its original value; the film conductivity can be reversibly switched. The hysteresis between the negative and positive potential scans indicates that even at the slow potential scan rates employed, the film does not attain equilibrium. The counterion mobility may partially limit film switching. This dynamic method, when refined, may ultimately give, however, a better picture of the relative magnitudes of intermediate potential conductivities, since the degree of contact between film and electrode is kept more nearly constant. Also, dynamic observations on conductivity changes during film discharge and changes in film oxidation state may be important in designing conducting polymer-based batteries and in other uses exploiting the polymer's electrical properties<sup>10</sup>.

Chemical Charge Assay Experiments. The twin electrode thin layer cell experiment, schematically illustrated in Figure 5, proceeds (as described in

Experimental) by: (i) electrochemically charging the polymer film to a chosen potential via its underlying electrode, (ii) establishing a steady-state current between the two working electrodes for the redox titrant, then (iii) disconnecting the polymer coated electrode so that (iv) the polymer is discharged by oxidizing or reducing the redox titrant. As the polymer discharges, current flows at the naked electrode to re-reduce or re-oxidize redox titrant; the current thus reflects the film discharge. When the discharge is complete and the current has decayed, at the new equilibrium the polymer film has (in principle) been discharged from the oxidation state of its initial potential to that which would be attained by applying the potential of the naked electrode to the film.

To illustrate the experiment, Figure 6 shows the current-time transient obtained for the discharge of an initially oxidized, poly-[Os(bpy)<sub>2</sub>(vpy)<sub>2</sub>]<sup>3+</sup> film, by oxidizing the redox titrant [Ru(bpy)<sub>2</sub>Cl<sub>2</sub>]. For a period after disconnecting the polymer coated electrode, the current remains nearly diffusion limited by [Ru(bpy)<sub>2</sub>Cl<sub>2</sub>] transport. As the film nears complete reduction, the current falls off due to the decrease in poly-[Os]<sup>3+</sup> sites available for electron transfer. The current falls to zero as the polymer film and solution cavity are both charged to the potential of the naked electrode. The extra inflection in current at about eight seconds is probably an uncompensated resistance effect typical of thin layer cells when the current flows between an electrode in the thin layer cavity and an auxiliary electrode outside the cavity.

Integrating a current-time transient like that in Figure 6 gives an experimental charge Q representing: (i) the charge removed from the polymer, Q<sub>p</sub>, (ii) less the gradient dC<sub>p</sub>/dx, (if any) of charged sites existing across

the polymer film prior to disconnection, (iii) plus one-half the moles of redox titrant in the cell (its concentration times the volume of the thin layer,  $V = AL$ , where  $A$  is the electrode area, and  $L$  is the interelectrode distance; the thin layer contains roughly equal quantities of oxidized and reduced titrant before disconnection of the polymer electrode). This may be expressed:

$$Q = Q_p(1 - i_{ss}/2I_{ct}) + (nFALC_s/2)(i_{ss}/I_{mt}) \quad (2)$$

where  $i_{ss}$  is the measured steady state current prior to disconnection of the polymer electrode,  $I_{mt}$  is the current limited by mass transport of redox titrant across the thin solution layer<sup>28</sup>, and  $I_{ct}$  is the electron diffusion limiting current<sup>29</sup> (the maximum current the film can support). The  $(1 - i_{ss}/2I_{ct})$  term takes into account factor (ii), the possible existence of a gradient of charged sites across the film under steady-state conditions, which lowers the charge present in the film. When  $i_{ss}/2I_{ct}$  is small and negligible (the gradient of charged sites in the film is shallow), then  $i_{ss}/I_{mt}$  becomes unity. This is the case for the Os polymer film<sup>29</sup> studied in Figure 6, and since the poly(pyrrole) film can support currents much larger than  $I_{mt}$ ,  $i_{ss}/2I_{ct}$  is reasonably assumed negligible for it as well. Thus, eq. (2) becomes

$$Q = Q_p + nFALC_s/2 \quad (3)$$

and, the experimental charge is simply equal to the total polymer charge plus one half of the charge for consumption of redox titrant in the cell. Repeating the experiment at a series of initial polymer electrode potentials yields a plot of polymer charge ( $Q_p$ ) vs. initial polymer potential ( $E$ ).

The  $Q_p$  vs.  $E$  result (Figure 7B) for the chemical charge assay of poly- $[\text{Os}(\text{bpy})_2(\text{vpy})_2]^{3+}$  by  $[\text{Ru}(\text{bpy})_2\text{Cl}_2]$  ( $E^\circ = +0.3\text{V}$ ) has a typical Nernstian shape, confirming what is expected from the cyclic voltammetry of the polymer

(Figure 7A); no excess charge is stored in this polymer at potentials well positive of  $E^\circ$ . The  $Q_p$  vs.  $E$  curve is obviously equivalent to an integrated cyclic voltammogram, and the limiting  $Q_p$  from Fig. 7B, 774 mC, agrees with that obtained by integrating the actual cyclic voltammogram (Figure 7a), 787 mC. This simple experiment on a well understood polymer which conducts electrons by site-site hopping<sup>27</sup>, brings out the basic idea of the chemical charge assay. Application of the experiment to polymers showing anomalous voltammetry (such as poly(pyrrole)), to polymers which do not undergo facile electron-transfer with the electrode, or to those which exhibit slow or incomplete electron diffusion, should be useful.

Returning to poly(pyrrole), Figure 8B (left-hand axis) shows  $Q_p$  vs.  $E$  results for reduction of poly(pyrrole) by methyl viologen ( $MV^+$ ,  $E^\circ = -0.455$  V). Little if any charge is extracted from the film when its initial potential is more negative than  $-0.3$  V, near  $E^\circ$  for  $MV^{2+}/+$ . From  $-0.3$  V to approximately  $0$  V, some charge is extracted. From  $0$  V to  $+0.65$  V, the charge changes linearly with potential, indicating a constant poly(pyrrole) film capacitance of  $5.73$  mF/cm<sup>2</sup> over these potentials. The charge on poly(pyrrole) films at potentials well positive of its supposed voltammetric peak ( $E^\circ$  about  $-0.2$  V) is clearly available to do useful chemical work, as evidenced by its reaction with reduced methyl viologen.

The constant capacitance observed in Figure 8B is not well reflected in the  $20$  mV/s cyclic voltammetry, Figure 8A, of this film (typical of thick poly(pyrrole) films), but it is in voltammograms of much thinner films. The absence of a well defined reduction peak in the voltammetry (Figure 8A) also explains the absence in Figure 8B of a break in the  $Q_p$  vs.  $E$  curve like that shown in Figure 7B.

Results for charge assay oxidation of reduced poly(pyrrole) by  $[\text{Ru}(\text{bpy})_2\text{Cl}_2]^+$  are shown in Figure 8C. Note that the film could be charged only to approximately the formal potential of  $(\text{Ru}(\text{bpy})_2\text{Cl}_2)$ , 0.3 V. However, extrapolation of the linear segment of the curve to more positive potentials gives a total film charge (1.55 mC) which agrees closely with that obtained by the assay of Figure 8B. The "knee" (discontinuity in slope) in the  $Q_p$  vs. E curve may be correlated with the cyclic voltammetric oxidation wave (Figure 8A), which is better defined than is the reduction peak.

Taking into account film area and thickness, the constant poly(pyrrole) film capacitance at potentials more positive than 0V corresponds from the chemical charge assay data of Figures 8B and 8C to bulk capacitances of 356 and 203  $\text{F}/\text{cm}^3$ , respectively. If we alternatively evaluate the poly(pyrrole) capacitance by the more conventional electrochemical procedure of stepping the potential of the electrode upon which it is coated between 0.1 and 0.5V and integrating the current flow until background is reached, values of 211 and 225  $\text{F}/\text{cm}^3$  are obtained for positive and negative-going steps, respectively. Integration of cyclic voltammograms over these potentials<sup>18c</sup> gives 240  $\text{F}/\text{cm}^3$ , and bulk capacitance values by AC impedance measurements are (131  $\text{F}/\text{cm}^3$ )<sup>18c</sup> and (100 $\text{F}/\text{cm}^3$ )<sup>13,20</sup>.

There is a spread of nearly a factor of 4X between these differently determined bulk capacitances, which appears larger than experimental uncertainty. The differences suggest that discharge over a longer timescale (chemical assay and potential steps) is capable of extracting more charge from the poly(pyrrole) than more rapid discharge (AC impedance). The data also indicate that, on roughly equal timescales, the reducing titrant  $\text{MV}^+$  is able to sample more of the charge stored on oxidized poly(pyrrole) than can an



electrode underlying a film of oxidized or reduced poly(pyrrole). The oxidant  $[\text{Ru}(\text{bpy})_2\text{Cl}_2]^+$  and an underlying electrode appear equally efficient at oxidizing a reduced poly(pyrrole) film. These comparisons clearly indicate that significant heterogeneity can exist between the discharge rates of different parts of poly(pyrrole) films. The data give no direct basis to speculate on the physical or chemical nature of the heterogeneity, except it seems obvious that the electrically insulating nature of the reduced material could be important in some circumstances.

It is of interest to express the chemical charge assay ( $Q_p$ ) data in terms of the fractional charge ( $q_{\text{mon}}$ ) associated with each pyrrole subunit at a given potential. This is done through the following manipulation:

$$q_{\text{mon}} = 2Q_p / (Q_d - Q_{d,p} - Q_{\text{sol}}) \quad (4)$$

where  $Q_d$  is the amount of charge passed during electropolymerization of the poly(pyrrole),  $Q_{d,p}$  is the chemical charge hypothetically available from a film oxidized to the potential used for electropolymerization (0.83V), obtained by (\*\*\*\*) extrapolation of the  $Q_p$  vs. E curve of Figure 8B, and  $Q_{\text{sol}}$  is the charge due to soluble poly(pyrrole) oligomers which escape from the film during electropolymerization (which we assume negligible here). Equation 4 also assumes that  $2+q_d$  electrons are required to polymerize each pyrrole unit (where  $q_d$  electrons are required to charge each poly(pyrrole) subunit up to the electropolymerization potential)<sup>15</sup>. Note that  $q_{\text{mon}}$  evaluated in this way does not rely on the previously established relationship<sup>15</sup> between deposition charge and polymer film thickness.

The right-hand axis of Figure 8B shows the charge assay  $Q_p$  data of Figure 8B (left hand axis) converted with Eq. 4 to  $q_{\text{mon}}$  as a function of potential. The partial charge, and therefore the number of counterions, associated with

each pyrrole subunit, is potential dependant. Of interest in this regard is the fact that the composition of oxidized poly(pyrrole) has previously been discussed<sup>16,30</sup> in terms of a static stoichiometric pyrrole subunit/counterion ratio. Based on elemental analyses of freshly polymerized, unperturbed films, the pyrrole/counterion ratio was assigned values of 4/1 for the fluoroborate salt<sup>30</sup>, and 3/1 for the perchlorate salt<sup>16</sup>. Figure 8B suggests on the other hand, that the actual counterion concentration of poly(pyrrole), and thus the elemental analysis for anion concentration, must vary with the electropolymerization potential used in film preparation, and that no fundamentally unique pyrrole/counterion ratio exists. More positive polymerization voltages may result in higher apparent anion concentrations. Extrapolation of the  $q_{\text{mon}}$  vs. E curve to 0.83V (our electropolymerization potential) gives a  $q_{\text{d}}$  value of approximately 0.38, or slightly less than three pyrrole subunits per perchlorate anion at that potential.

Finally, we consider the correlation of the  $q_{\text{mon}}$  potential profile of Figure 8B with the conductivity/potential profile of Figure 2. Combining these Figures produces the important result of Figure 9, showing how conductivity depends on the fractional charge of each poly(pyrrole) unit. At very low fractional charges, the mostly reduced, undoped films are poor conductors. At intermediate fractional charges (0-0.15) the conductivity increases more or less linearly with charge, and then at about  $q_{\text{mon}} = 0.15$ , reaches a limiting conductivity after which additional oxidation of the film has no effect on conductivity. On the potential axis, reference to Figures 2 and 8B shows that the limiting conductivity is attained at about 0.2 or 0.1V vs. SSCE.

Qualitatively, Figure 9 agrees with results by Street, et al<sup>24,25</sup>, on the (dry) conductivity of slightly (gas phase) oxidized poly(pyrrole).

Quantitatively, our data suggest that solvent-wetted poly(pyrrole) reaches full conductivity at roughly  $q_{\text{mon}} = 0.15$ , or at one electron "hole" (and counterion) for about every seven pyrrole subunits. This result is a somewhat higher degree of oxidation than observed in the gas phase experiment by Street, et al (0.04 fractional oxidation<sup>20</sup>). The needed degree of oxidation is small, in either case.

Feldberg<sup>20</sup> has discussed Street's<sup>24,25</sup> observation in terms of double layer charging voltammetry of a porous poly(pyrrole) film with high surface to volume ratio as suggested by Bull, Fan and Bard's results<sup>13</sup>. This model is quite appealing, but let us consider the consequences of assuming that the surface pyrrole units supply all of the electrons withdrawn from the microporous polymer. (Whether considered as "faradaic" or "non-faradaic",  $q_d$  electrons are extracted from the polymer as discussed above.) Based on rod-shaped fibrils and a  $2 \times 10^{-5}$  F/cm<sup>2</sup> differential capacitance, Feldberg<sup>20</sup> estimates that a 4 nm rod radius would supply a 100 F/cm<sup>3</sup> bulk capacitance. If the capacitance actually exceeds 200 F/cm<sup>3</sup>, as our data show, 2 nm rod radii are required. From these pictures, 23 or 44%, respectively, of all of the pyrrole sites must lie within 0.5 nm (about a site dimension) of the rod's polymer/solution interface, and these sites must yield a sufficient and uniform density of surface states to accommodate the oxidative electron loss of the charging process. The value of  $q_d = 0.3$  at +0.5V (Figure 8B) is indeed large enough to be consistent with this picture. On the other hand, the degree of microporosity required to satisfy the huge poly(pyrrole) bulk capacitance is so extreme that we believe the alternative picture, of a more spatially uniform charging of pyrrole sites throughout a relatively less porous polymer volume, remains equally appealing and cannot be ruled out. The number of electrons

withdrawn from a poly(pyrrole) band having a relatively uniform density of states, and the number of charge compensating counterions, is the same in either picture.

In summary, the electrical conductivity of poly(pyrrole) appears to depend on the state of polymer charge only at potentials negative of 0.1 to 0.2V. At more positive potentials, conductivity is unaffected, even though the film has a capacity for considerable further charging. Whatever the chemical nature of the changes that occur at potentials more positive than +0.1 to 0.2V, they apparently do not significantly alter the structural features of poly(pyrrole) that determine its electrical conductivity.

The potential dependency of the ionic conductivity of poly(pyrrole) seems to parallel the electrical conductivity. That is, the most striking changes in ionic conductivity<sup>18</sup> also occur at potentials more negative than about 0V, and so the chemical event(s) that lead to major changes in ionic and electrical conductivity appear to be related. In the simplest of interpretations, a reduced poly(pyrrole) chain (or ensemble thereof) becomes electrically conducting by becoming oxidized and cationic; the latter property in turn produces a permeability of the polymer structure to anionic counterions.

Finally, the non-linear relationship between poly(pyrrole) conductivity and charge (oxidation state) expressed in Figures 2 and 9 suggests that poly(pyrrole) electrical conductivity may be determined by different limiting factors depending on the film oxidation state. The various conductivity controlling factors which have been suggested include the population of bipolarons<sup>32,33</sup>, the percentage of chains or segments thereof which are oxidized (chain oxidation state being a function of chain length at a given potential)<sup>31</sup>, and the rate of electron hopping between chains or across chain

defects<sup>34</sup>. The result of Figure 9 thus suggests a possible shift of control between two of the above (or some other) factors.

Acknowledgement. This research was supported in part by grants from the National Science Foundation and the Office of Naval Research.

## References

1. Chang, C. K.; Druy, M. A.; Gau, S. C.; Heeger, A. J. Louis, E. J.; MacDiarmid, A. G.; Park, Y. W.; and Shiraka, H., J. Am. Chem. Soc., 1978, 100, 1013.
2. Kanazawa, K. K.; Diaz, A. F.; Geiss, R. H.; Gill, W. D.; Kwak, J. F.; Logan, J. A.; Rabott, J. F.; and Street, G. B., J. Chem. Soc. Chem. Commun., 1974, 854.
3. Yamamoto, T.; Sanechica K.; and Yamamoto, A., J. Polym. Sci., Polym. Lett. Ed., 1980, 18, 9.
4. Shacklette, L. W.; Chance, R. R.; Ivory, D. M.; Miller, G. G.; and Baughman, R. H. Baughman, Synth. Met. 1979, 1, 307.
5. Chance, R. R.; Shacklette, L. W.; Eckhardt, H.; Sowa, J. M.; Elsenbaumer, R. L.; Ivory, D. M., Miller, G. G.; and Baughman, R. H.; ACS Meeting, San Francisco, August, 1980.
6. Wnek, G. E.; Chien, J. C. W.; Karasz, F. E.; and Lillya, C. P., J. Polym. Sci., Polym. Lett. Ed., 1979, 20, 1441.
7. Nigrey, P. J.; MacDiarmid, A. G.; and Heeger, A. J., J. Chem. Soc. Chem. Commun., 1979, 594.
8. Heeger, H. G.; and MacDiarmid, A. G. in "The Physics and Chemistry of Low Dimensional Solids", L. Alacer, Ed., 353-397, P. Reidel, 1980.
9. Noufi, R.; Tench, D.; and Warren, L. F., J. Electrochem. Soc., 1981, 128, 2596
10. Kittlesen, G. P.; White, H. S.; and Wrighton, M. S., J. Am. Chem. Soc., in press.
11. Hug, R.; and Farrington, G. C., J. Electrochem. Soc., 1984, 131, 819.

12. Diaz, A. F.; Vasquez Vallejo, J. M.; and Duran, A. M., IBM J. Res. Develop., 1981, 25, 42.
13. Bull, R. A.; Fan, R. F.; and Bard, A. J., J. Electrochem. Soc., 1982, 129, 1009.
14. Diaz, A. F.; Castillo, J. I.; Logan, J. A.; and Lee, W. Y., J. Electroanal. Chem., 1981, 129, 115-132
15. Diaz, A. F.; and Castillo, J. I., J. Chem. Soc. Chem. Commun., 1980, 397.
16. Kanazawa, K. K.; Diaz, A. F.; Gill, W. D.; Grant, P. M.; Street, G. B.; Gardini, G. P.; and Kwak, J. F., Synthetic Metals, 1979/80, 1, 329.
17. Tourillon G.; and Garnier; F., J. Phys. Chem., 1983, 87, 2289.
18. (a) Burgmayer, P.; and Murray, R. W., J. Am. Chem. Soc., 1982, 104, 6139; (b) Burgmayer, P.; and Murray, R. W., J. Phys. Chem., 1984, 88, 2515; (c) Burgmayer, P.; and Murray, R. W. in preparation.
19. Anderson, L. B.; and Reilley, C. N., J. Electroanal. Chem., 1965, 10, 295-305.
20. Feldberg, S., J. Am. Chem. Soc., 1984, 106, 4671.
21. Yakushi, K.; Lauchlan, L. J.; Clarke, T. C.; and Street, G. B., J. Chem. Phys. 1983, 79, 4774.
22. Dwyer, F. P.; Goodwin, E. C.; and Gyarfas, E. C. Aust. J. Chem., 1963, 16, 544.
23. Calvert, J. M.; Schmehl, R. H.; Sullivan, B. P.; Facci, J. S.; Meyer, T. J.; and Murray, R. W., Inorg. Chem., 2151, 22, 2151.
24. Pfluger, P.; Krounbi, M.; Street, G. B.; and Weiser, G. J., J. Chem. Phys., 1983, 78, 3212.
25. Scott, J. C.; Pfluger, P.; Krounbi, M. T.; and Street, G. B., Phys. Rev. B., 1983, 28, 2140.

26. Genies, E. M.; Bidan, G.; and Diaz, A. F., J. Electroanal. Chem., 1983, 149, 101 (1983).
27. Kaufman, F. B.; Schroeder, A. H.; Engler, E. M.; Kramer, S. R.; Chambers, J. Q., J. Am. Chem. Soc., 1980, 102, 483.
28.  $I_{mt} = nFADC/L$  for a twin electrode thin layer cell at steady state<sup>17</sup>, assuming the diffusion coefficients for the oxidized and reduced species are equal. The correction term,  $i_{ss}/I_{mt}$ , is assumed to be unity.
29.  $I_{ct} = nFAD_{ct}C_p/d$  where  $D_{ct}$  is the rate constant for electron diffusion,  $C_p$  is the concentration of charged sites in the polymer, and  $d$  is the film thickness.  $D_{ct}$ , obtained previously, is  $5 \times 10^{-9} \text{ cm}^2/\text{s}$ , and  $d$  is calculated from a knowledge of film density and quantity of electroactive sites. For the Os film, the  $1 - i_{ss}/2I_{ct}$  term in equation (2) equals 0.995.
30. Street, G. B.; Clarke, T. C.; Krounbi, M.; Kanazawa, K.; Lee, V.; Pfluger, P.; Scott, J. C.; and Weiser, G., Mol. Cryst. Liq. Cryst., 1982, 83, 253.
31. Bredas, J. L.; Silbey, R.; Boudreaux, D. S.; and Chance, R. R., J. Am. Chem. Soc., 1983, 105, 6555
32. Bredas, J. L.; Themans, B.; and Andre, J. M., Phys. Rev. B., 1983, 27, 7827.
33. Scott, J. C.; Pfluger, P.; Krounbi, M. T.; and Street, G. B., Ibid., 1983, 28, 2140 (1983).
34. Tanaka, M.; Watanabe, A.; Fujimoto, H.; and Tanaka, J. and Mol. Cryst. Liq. Cryst., 1982, 83, 277.



## Figure Legends

Figure 1. Schematic illustration of twin electrode thin layer cell used for "static" conductivity measurements.

Figure 2. Plot of log poly(pyrrole) film conductivity ( $\sigma$ ) vs. polymer potential (E) for a 10 mV potential difference applied across a 13.9 micron thick poly(pyrrole) film in 0.1M  $\text{Et}_4\text{NClO}_4/\text{CH}_3\text{CN}$ .

Figure 3. Plot of log poly(pyrrole) film conductivity ( $\sigma$ ) vs. potential drop ( $\Delta E$ ) across a 13.9 micron thick poly(pyrrole) film in 0.1M  $\text{Et}_4\text{NClO}_4/\text{CH}_3\text{CN}$  at various mean polymer potentials: (O) +0.38V, (O) -0.02V, ( $\Delta$ ) -0.22V, ( $\Delta$ ) -0.32V, ( ) -0.42V.

Figure 4. Plot of current density (J) vs. polymer potential (E) for a "dynamic" conductivity measurement on a small area ( $3.1 \times 10^{-4} \text{cm}^2$ ) 13.3 micron thick poly(pyrrole) film in 0.1 M  $\text{Et}_4\text{NClO}_4/\text{CH}_3\text{CN}$ .  $\Delta E = 10 \text{ mV}$ , sweep rate =  $1 \text{ mVs}^{-1}$ .

Figure 5. Schematic illustration of twin-electrode thin layer cell chemical charge assay measurement. R and Ox are reduced and oxidized forms, respectively, of a soluble "redox titrant".

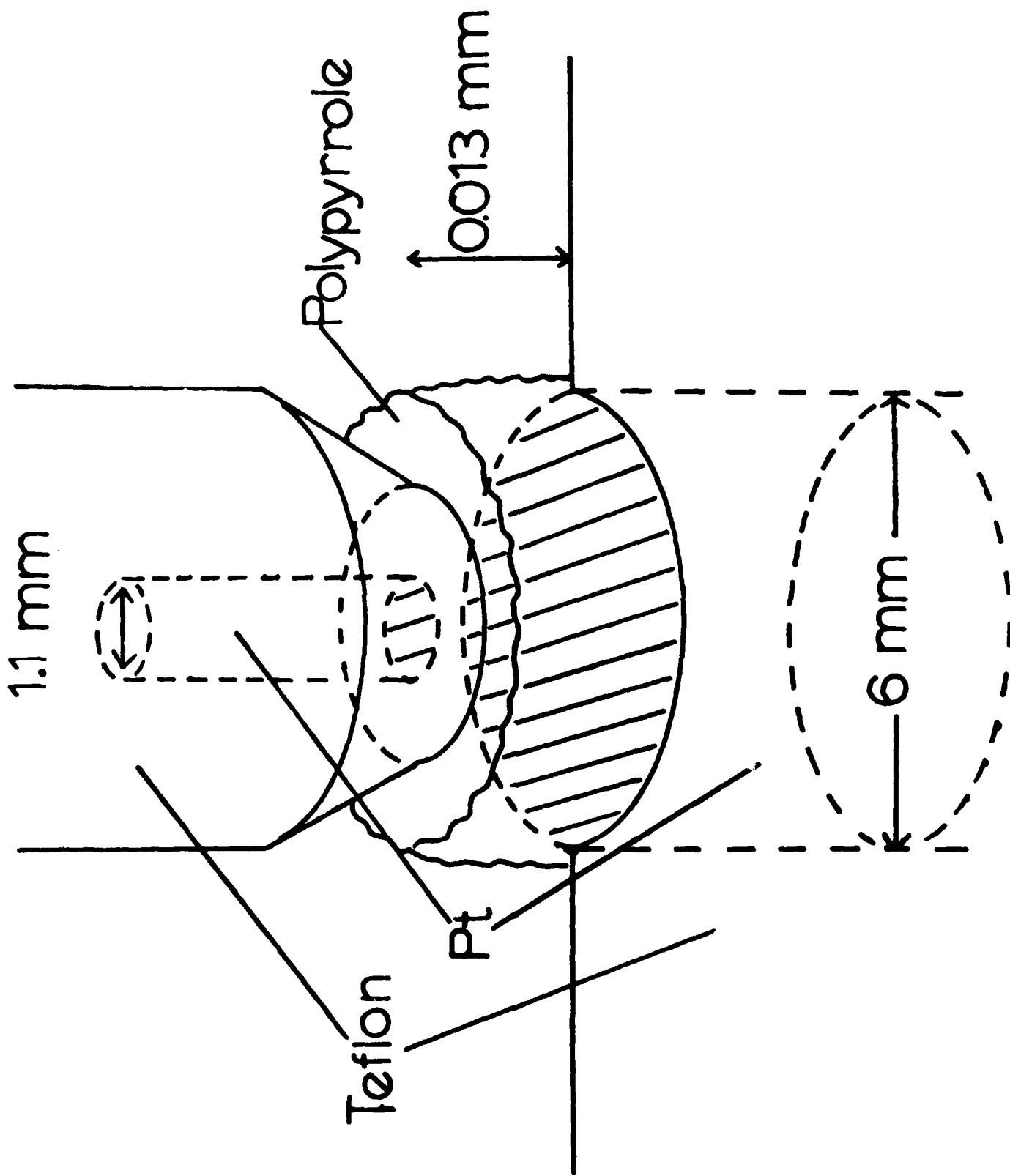
Figure 6. Current-time transient for reduction of a poly-[Os(bpy)<sub>2</sub>(vpy)<sub>2</sub>]<sup>3+</sup> film by 0.88 mM [Ru(bpy)<sub>2</sub>Cl<sub>2</sub>] in 0.1 M  $\text{Et}_4\text{NClO}_4/\text{CH}_3\text{CN}$ . Polymer coated electrode potential 1.0V; naked electrode potential 0V; electrode separation 36.6 microns.  $i_{ss}$  is the steady state limiting current prior to polymer coated electrode disconnection.

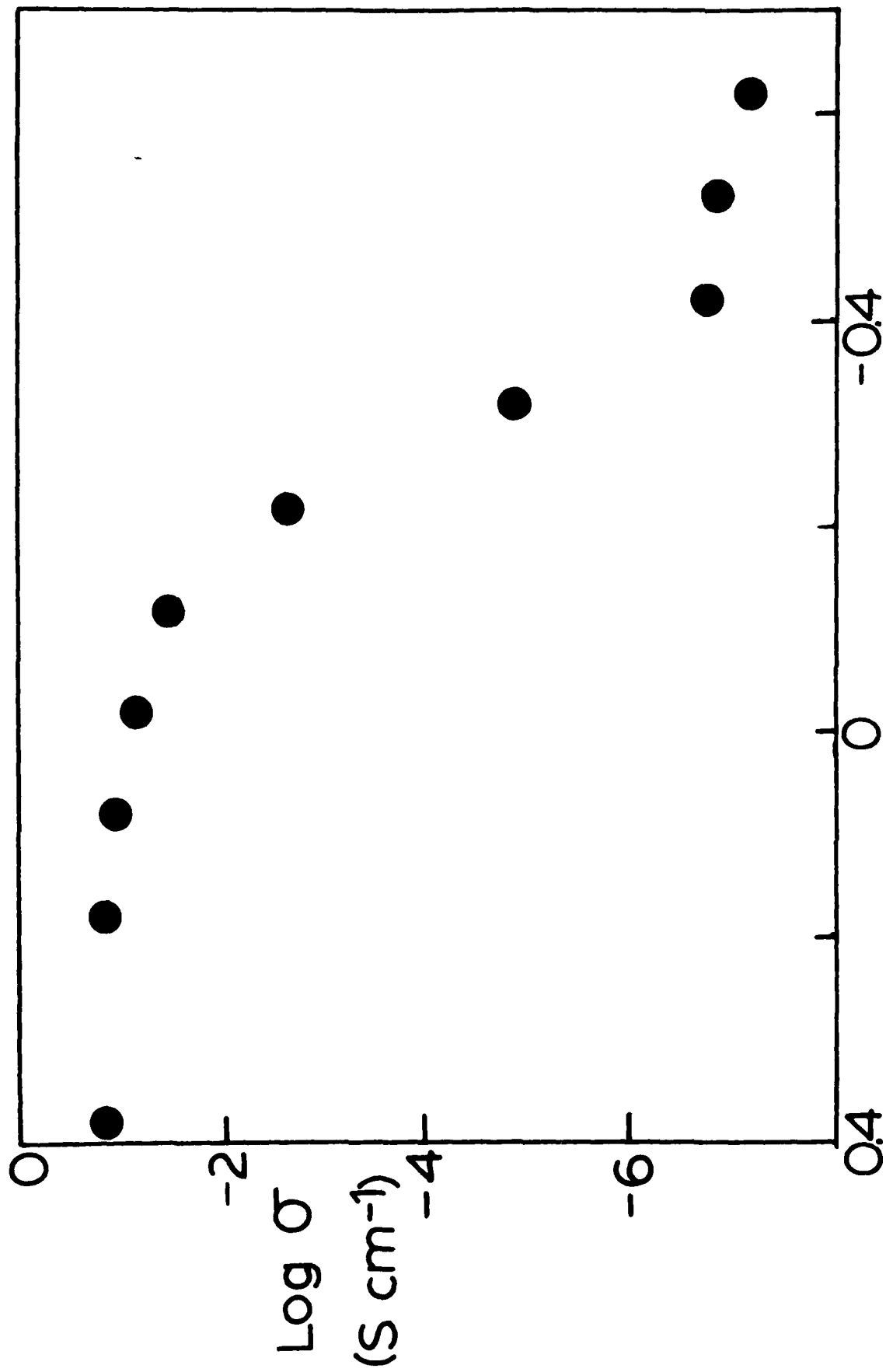
Figure 7. Chemical charge assay of poly-[Os(bpy)<sub>2</sub>(vpy)<sub>2</sub>] film in 0.1M  $\text{Et}_4\text{NClO}_4/\text{CH}_3\text{CN}$ . A; cyclic voltammetry, sweep rate =  $20 \text{ mV s}^{-1}$ . B; plot of polymer charge ( $Q_p$ ) for reduction by 0.88 mM [Ru(bpy)<sub>2</sub>Cl<sub>2</sub>] as in Figure 6,

vs. polymer potential (E). Naked electrode potential 0V; electrode separation = 36.6 microns.

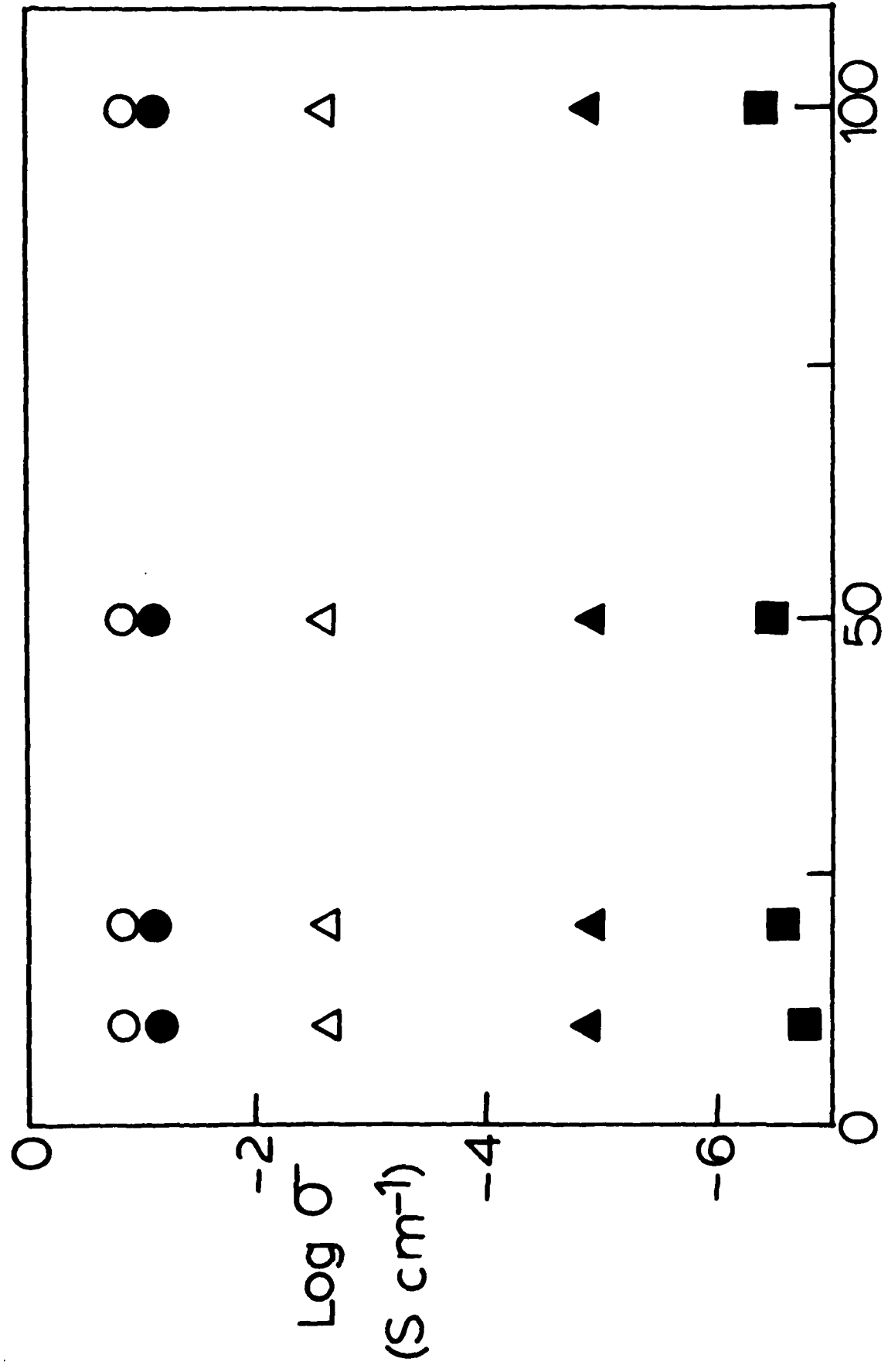
Figure 8. Chemical charge assay of poly(pyrrole) film in 0.1 M  $\text{Et}_4\text{NClO}_4/\text{CH}_3\text{CN}$  prepared with 10 mC deposition charge. Panel A: cyclic voltammetry with sweep rate =  $20 \text{ mV s}^{-1}$ . Panel B: plot of poly(pyrrole) charge ( $Q_p$ , left-hand axis) and fractional charge per pyrrole monomer subunit ( $q_{\text{mon}}$ , right-hand axis) vs. poly(pyrrole) coated electrode potential (E), obtained by reduction with  $1.16 \text{ mM MV}^+$ . Naked electrode potential  $-0.6\text{V}$ ; electrode separation 58.9 microns; note extrapolation ('''') of linear portion to polymerization potential (0.83V). Panel C: Poly(pyrrole) charge ( $Q_p$ ) vs. polymer potential (E) obtained by oxidation with  $1.05 \text{ mM [Ru(bpy)}_2\text{Cl}_2]$ . Naked electrode potential 0.4V; electrode separation 35.1 microns.

Figure 9. Plot of poly(pyrrole) conductivity ( $\sigma$ ) vs. fractional charge per pyrrole monomer subunit ( $q_{\text{mon}}$ ) in 0.1 M  $\text{Et}_4\text{NClO}_4/\text{CH}_3\text{CN}$ .





$E/V$  vs. SSCE



$\Delta E$  (mV)

